Volume 1 | Number 1 | Jan 2013 | Pages 1–100

Journal of
Materials Chemistry A

Materials for energy and sustainability
www.rsc.org/materialsA

ROYAL SOCIETY
OF CHEMISTRY

ROYAL SOCIETY
OF CHEMISTRY

www.rsc.org/materialsA

ROYAL SOCIETY OF CHEMISTRY

Journal Name

ARTICLE

Carbohydrate based hypercross-linked organic polymers with –OH functional group for CO$_2$ separation†

Haiying Li, [#a, b] Bo Meng, [#c] Shannon M. Mahurin,[b] Songhai Chai,[c] Kimberly M. Nelson,[c] David C. Baker,[c] Honglai Liu[*a] and Sheng Dai[*b, c]

Recently, microporous organic polymers, especially those hypercross-linked from functionalized aromatic monomers, have shown to be effective for CO$_2$ capture and storage with considerable capacity and selectivity. Herein, a class of novel microporous hypercross-linked polymers (HCPs), based on green and renewable carbohydrates, was synthesized by Friedel−Crafts alkylation for carbon capture and storage by hydrogen bonding and dipole−quadrupole interaction. These carbohydrate polymers, which have BET surface areas around 800 m^{2}g^{-1}, can absorb considerable amount of CO$_2$ with the CO$_2$/N$_2$ selectivity up to 42 at 273 K, and 96 under 100 kPa in the mixed gases (0.15 mol CO$_2$, 0.85 mol N$_2$). Furthermore, we experimentally and computationally studied the structures of carbohydrate backbones and determined several features that govern their CO$_2$ absorption ability, which sheds light on understanding the structure/function relationship for designing better CO$_2$ separation materials.

Introduction

Anthropogenic CO$_2$ is one of the primary atmospheric greenhouse gases with a significant contribution to global climate change and long-term negative effects on the environment.[1] Consequently, the ability to capture and store CO$_2$ from combustion exhausts and other sources is critical for managing future climate risks.[2] Over the years, much effort[3] has been devoted to the design and fabrication of functional materials for CO$_2$ capture. One promising approach has been the design and synthesis[4] of microporous organic polymers (MOPs) which has attracted considerable attention because of their high permanent microporosity and physicochemical stability.[5] Recently, the application of Friedel–Crafts alkylation of aromatic CO$_2$-philic moiety monomers was demonstrated via the "knitting" of MOPs.[6] The networks are derived from the high cross-linking of the polymer monomers whose inefficient packing of rigid and contorted components leads to an open microporous structure.[7] While the realization of this strategy is significant,[6] the vast majority of porous hypercross-linked polymers (HCPs) described to date are composed of aromatic-based skeletons derived from non-renewable petrochemical feedstock that do not readily degrade, which could potentially

cause additional environmental issues. Therefore, the synthesis of cost-effective and environmentally friendly MOPs remains an important challenge.

To address this challenge, we designed and synthesized a series of novel hypercross-linked carbohydrate MOPs for CO$_2$ capture and storage. Carbohydrates are ubiquitous in nature and play many varied and essential roles in a wide range of processes in living systems.[8] Their wide availability and properties such as renewable and sustainable character, tunable polarity, mechanical properties, and biodegradability,[9] along with their affinities[10] with lectins, lipids and carbohydrates, have led to significant development in the synthesis of carbohydrate-based materials in various applications such as reaction catalysis,[11] drug discovery and delivery[12] and virus detection.[13] The six-membered pyranose ring structure is the most representative monosaccharide structure, generally with a large number of attached hydroxyl groups. This implies a weak nucleophilicity and the potential to physisorptively bind CO$_2$ by means of a dipole–quadrupole interaction as well as the formation of hydrogen bonds.[14] Moreover, each sugar could work as a "functional group base station" with its hydroxyl groups either flexibly and regioselectively retained or substituted with alternate polar functional groups, which are critical in selective CO$_2$ capture.[15] Very recently, Stoddart and coworkers reported γ-cyclodextrin-based metal-organic framework (MOF) materials for CO$_2$ capture and demonstrated the formation of a carbonate with orientated primary hydroxyl groups on the C-6 position[14,16] of each glucose unit on γ-cyclodextrin.[17]

Herein, we report the polymerization of various benzylated carbohydrates with/without a free hydroxyl group at the C-6 position in the monosaccharide form using formaldehyde

[a.] State Key Laboratory of Chemical Engineering and Department of Chemistry, East China University of Science and Technology, Shanghai, 200237, China. Email: hlliu@ecust.edu.cn
[b.] Chemical Science Division, Oak Ridge National Laboratory, Oak Ridge, TN, 37831, United States. Email: dais@ornl.gov
[c.] Department of Chemistry, University of Tennessee, Knoxville, TN 37996, United States.
[#] These authors contributed equally to this work.
† Electronic Supplementary Information (ESI) available: experimental details, characterization figures and computational details. See DOI: 10.1039/x0xx00000x
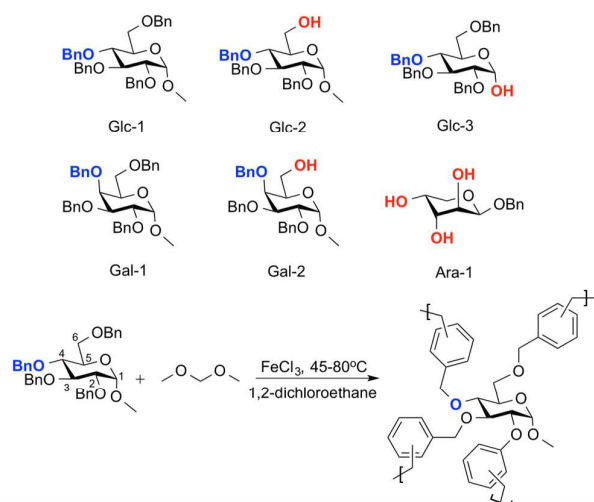
Scheme 1. Structures of featured benzylated carbohydrate monomers and representative polymerization by Friedel–Crafts alkylation.

dimethyl acetal (FDA) in a Friedel–Crafts alkylation hypercross-linking process. We initially prepared and synthesized a series of benzylated carbohydrate monomers including glucosides (Glc), galactosides (Gal) and an arabinoside (Ara), which featured several typical carbohydrate skeletons (Scheme 1). These carbohydrate monomers were prepared in a hierarchical fashion: Glc-1 and Gal-1 were directly benzylated[18] from methyl α-D-glucopyranoside and methyl α-D-galactopyranoside, respectively, without any free hydroxyl group; Glc-2, Gal-2 and Glc-3 were selectively benzylated, with either one primary (Glc-2 and Gal-2) or secondary hydroxyl group (Glc-3) left free. Ara-1 was only benzylated on the anomeric position with most of its hydroxyl groups left free. This regioselective benzylation protocol allows for facile hypercross-linking polymerization by Friedel–Crafts alkylation[19, 6b] with an external cross-linker and easy expansion of their functionality by incorporating one or several hydroxyl groups that would facilitate their CO_2 absorption ability.

Experimental and computational section

General carbohydrate monomer synthesis

All chemicals were purchased as reagent grade and used without further purification, unless otherwise noted. Reagent grade dichloromethane (CH_2Cl_2), tetrahydrofuran (THF), methanol (MeOH) and N, N-dimethylformamide (DMF) were obtained from the Pure-Solv (Innovation Technologies) solvent system that uses alumina columns, except for DMF, which was dried over a column of 5Å molecular sieves. Pyridine was distilled over CaH_2 prior to use. All reactions were performed under anhydrous conditions unless otherwise noted. Reactions were monitored by thin-layer chromatography (TLC) on silica gel precoated aluminum plates. Zones were detected by UV irradiation using a 254 nm lamp and/or by heat/charring with p-anisaldehyde–sulfuric acid development reagent. Column chromatography was performed on silica gel (40–63 μm). ^1H and ^{13}C NMR spectra were recorded at room temperature with a Varian VNMRS 500 MHz or a Varian VNMRS 600 instrument. Chemical shifts are reported in δ-units (ppm) relative to the residual ^1H $CDCl_3$ at δ 7.26 ppm and ^{13}C at δ 77.16 ppm. Mass spectrometric analysis was performed on a QSTAR Elite quadrupole time-of-flight (QTOF) mass spectrometer with an ESI source. Compounds Glc-3 and Ara-1 were purchased from Sigma–Aldrich and compound Gal-1 was purchased from Santa Cruz Biotechnology. Compounds Glc-1[S1], Glc-2[S2], and Gal-2[S2] are synthesized on the base of literature procedures.

General polymerization of benzylated carbohydrates

Typically, to a solution of the monomer and FDA in anhydrous 1,2-dichlorehane, a slurry of $FeCl_3$ in DCE was slowly added under nitrogen atmosphere. The mixture was then heated to 45 °C for 5 h and 80 °C for 19 h. The resulting brown precipitate was collected and washed with methanol and water until the filtrate became colorless and further purified by Soxhlet Extraction with methanol for 24 h. The polymer was dried under vacuum for 24 h at 60 °C. For different monomers, the ratio of external cross-linker FDA and catalysis $FeCl_3$ was adjusted because of the diverse numbers of benzyl rings as illustrated in Table S1.

Computational details

Quantum chemistry calculations were performed based on DFT method by G09 program. Since the calculation processes are expensive and time-consuming, basic monomers with simplified structures were applied in the assessment of each type of hyper cross-linked polymers (Figure S6). The geometries of all the monomer and monomer–gas pairs were fully optimized with M062x/6-311g(d, p) method, which is one of the most popular DFT methods in the study of intermolecular interactions. Frequency calculations at the same level were also performed to make sure all optimized structures could represent the actual minimum potential energy. Moreover, all the interaction calculations were corrected with the basis set superposition error (BSSE) by Boys and Bernardi's procedure. In the initial analysis of CO_2–carbohydrate pair systems' geometries, both hydrogen bonding and dipole–quadrupole interactions were considered as initial structures (Figure S7). The binding energy between carbohydrate and gases was calculated by the following formula:

$$\Delta E = E(gas - monomer) - E(gas) - E(monomer) + E(BSSE)$$

(See supporting information for experimental and computational details.)

Results and discussion

The backbones of successfully synthesized HCPs were confirmed by FTIR and the structures were verified by solid-state ^{13}C NMR cross-polarization magic angle spinning nuclear magnetic resonance spectroscopy (CP-MAS NMR), (Figure S1). The CP-MAS NMR gave resonance signals at 130, 60–70, and 40–50 ppm. The peak at 60–70 ppm corresponds to the carbohydrate backbone in the polymer while the remaining peaks can be attributed to aromatic carbons and linkers,

respectively. In addition, the broad X-ray powder diffraction (XRD) spectra confirmed that all of the HCPs were amorphous (see Figure S2). Analysis of thermal stability was carried out by thermal gravimetric analysis (TGA) on the amorphous HCPs (Figure S3). Notably, even though carbohydrate monomers are not regarded as highly stable at high temperature, these carbohydrate HCPs show excellent thermal stability comparable to custom HCPs[4e], retaining more than 60–70 % of their mass even at 800 °C.

The porosity was investigated by nitrogen adsorption analysis at 77 K. As shown in Figure 1, the fully reversible isotherms of most HCPs represent type I isotherms with steep nitrogen uptake at low pressure and limited micropore distribution, except for Gal-2, which shows a type II isotherm indicating nitrogen condensation in the mesopore/macropores of Gal-2. This is not uncommon in hydroxyl-containing porous polymers.[6a] Clearly, the six-membered pyranose ring structure is rigid enough to form microporous polymers with high BET surface area and narrow pore range, which is similar to previously reported HCPs (Table 1), in line with the pore size distribution and TEM images of representative carbohydrate-based HCPs (Figure 1).[4e] The Ara-1 polymer exhibits the lowest BET surface area (470 $m^2 g^{-1}$) and smallest pore volume (0.30 $cm^3 g^{-1}$), because there is only one aromatic ring for hypercross-linking in each unit. Although Gal-2 shows the highest BET surface area, it has the smallest micropore percentage but wide micro and meso-pore distributions. We attribute this to a steric effect since the C–O bond on C-4 of the galactoside epimer is axial, and all the benzyl groups on C-2, C-3 and C-4 are oriented in different directions, which lead to less intensive hypercross-linking. However, it is still notable that the slight change of benzylated degree in the carbohydrate monomer has a negligible impact on the surface area, especially on the micropore surface area/volume (Table S1). In order to investigate the stability of HCP's pores in moisture and acidic conditions, all samples were soaked in water at pH=5 at 80°C for 48 hours and dried overnight at 80°C. The BET surface areas of all these samples remain over 87%, which makes it possible for industrial application (Table S2).

Because of the high BET surface areas of the carbohydrate polymers and the presence of -OH groups, we examined the CO_2 adsorption properties of the polymers up to 1 bar at 273 K and 298 K (Figure 2/S4, Table 1). At approximately 1 bar, most carbohydrate HCPs exhibit a CO_2 adsorption capacity greater than 10.1 wt% (2.30 mmol g^{-1}) and 5.89 wt% (1.34 mmol g^{-1}) at 273 K and 298 K, respectively, with perfectly reversible unsaturated isotherms. Compared with the hypercross-linked polymer of benzyl alcohol[4e] (8.46 wt%), which also has an, the alcohol hydroxyl group in the monomer carbohydrate HCPs show higher CO_2 adsorption ability with almost identical BET surface area. The BET surface area, particularly the micropore surface area, plays a significant role in determining the CO_2 uptake of the carbohydrate polymers, similar to other types of MOPs reported in previous work.[3a] For example, Ara-1 has the lowest BET surface area and adsorbs the smallest amount of

CO_2. However, Gal-2 possesses the highest BET surface area,
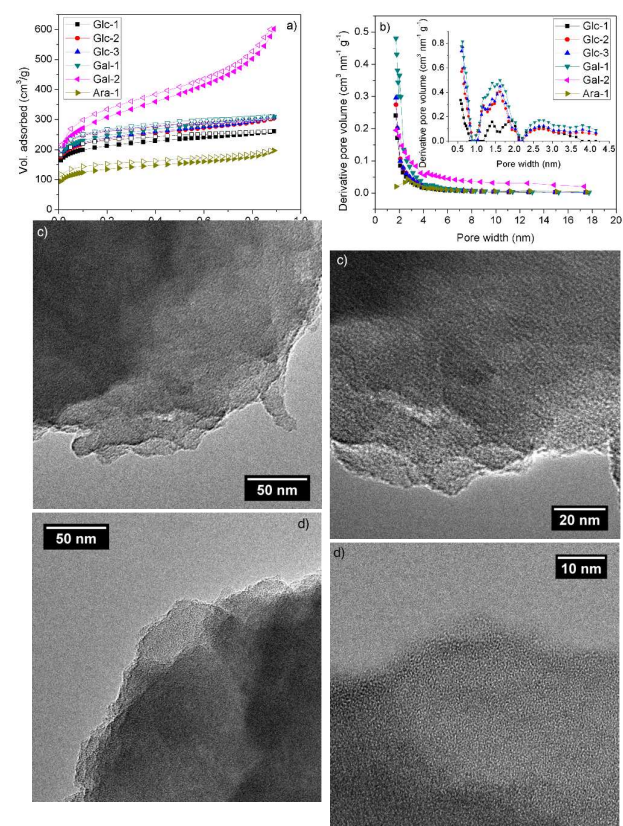
yet exhibits a CO_2 adsorption capacity similar to Glc-2 because

Figure 1. a) Nitrogen adsorption (solid symbols)–desorption (open symbols) isotherms at 77 K of samples. b) pore sizes distribution of six samples. c) TEM

Table 1. Characteristics and gas adsorption properties of carbohydrate HCPs.

Polymer	Surface area[a] (S_{BET})/ $m^2 g^{-1}$	Surface area[b] (S_L)/ $m^2 g^{-1}$	CO_2 uptake[c] cm^3(STP)/g (mmol g^{-1})		CO_2/N_2 selectivity (initial slope, 273 K/298 K)	Qst/ kJ mol^{-1}
			273 K	298 K		
Glc-1	735	970	51.3 (2.30)	29.9 (1.34)	25/18	27.9
Glc-2	816	1080	53.0 (2.36)	31.8 (1.42)	39/18	26.4
Glc-3	829	1096	54.0 (2.43)	33.0 (1.45)	41/27	25.8
Gal-1	858	1136	60.3 (2.70)	35.0 (1.57)	33/21	26.3
Gal-2	1090	1466	52.6 (2.35)	30.9 (1.38)	42/34	24.6
Ara-1	470	623	37.8 (1.69)	21.9 (0.98)	--/26	28.8

[a] Surface area calculated from nitrogen adsorption isotherms at 77 K by BET equation. [b] Surface area calculated from nitrogen adsorption isotherms at 77 K by the Langmuir equation. [c] Measured at a pressure of 1 bar.

images of Glc-1. d) TEM images of Gal-1.

of its limited micropore surface area. Moreover, Glc-1, Glc-2 and Glc-3 adsorb a similar amount of CO_2 because of their comparable micropore surface areas. As for fully benzylated carbohydrate polymers, the change of configuration from glucose to galactose slightly enhances the CO_2 adsorption capacity (Glc-1 10.10 wt% vs. Gal-1 11.90 wt%), in agreement with the galactose-based HCPs of higher BET surface area. Meanwhile, the heats of adsorption for all carbohydrate HCPs were calculated to be 25–28 kJ mol^{-1}, which is below the energy of chemisorptive processes (>44 kJ mol^{-1}), indicating strong physisorption and facile CO_2 release.

N$_2$ adsorption experiments were also carried out to calculate the CO_2/N_2 selectivity of these polymers. The selectivity was calculated in two ways. First, we used the slope of the CO_2 and N_2 isotherms at low pressure (i.e., in the Henry's law region) and calculated the ratio. Second, we determined the mixed gas selectivity based on the single gas isotherms using the ideal adsorbed solution theory at 0.15 mol CO_2, 0.85 mol N_2 and different pressures (see Supporting Information and Figures S5-6, Table S3 for details). The selectivity of these polymers ranges from 24 to 42 at 273 K, from 18 to 34 at 298 K (Table 1) and rose to 96 in the mixed gas calculation at 100 kPa, comparable with those benzene-based hypercross-linked polymers, and even better than some hydroxyl group functionalized HCPs such as 1-naphthol (16) and 1,1-bi-2-naphthol (26)[6a] under the same conditions (Table S4). Compared with the fully benzylated carbohydrate network, the polymers with free hydroxyl groups achieve higher CO_2/N_2 selectivity (Glc-1 vs. Glc-2/3 and Gal-1 vs. Gal-2). Interestingly, the secondary hydroxyl groups on C-1 of Glc-3 show stronger affinity with CO_2 than those primary hydroxyl groups on C-6 of Glc-2 under either 298 K or mixed gas system. Moreover, the selectivity can be clearly enhanced by changing the monomer structure from glucose to galactose. To be more specific, for benzylated carbohydrate polymers with/without hydroxyl groups on C-6, the selectivity of the galactose-based HCPs is higher than the glucose-based HCPs (Glc-1 vs. Gal-1, Glc-2 vs. Gal-2), especially in the mixed gas simulations.

The fact that galactose-based polymers exhibit better CO_2 capture performance than glucose-based polymers with a comparable framework indicates that the carbohydrate structure does affect both the CO_2 adsorption capacity and the CO_2/N_2 selectivity of the HCPs. In order to further explore the nature of the interactions between the carbohydrate polymers and gases, the effects of the –OH moieties in the framework on their affinity with CO_2 and N_2 was studied by quantum chemistry calculations with the M062x/6-311g(d, p) method[20] using G09 program.[21] It has been widely accepted that non-covalent interactions play a key role in CO_2 physisorption of MOPs. In this case, both hydrogen bonding and dipole–quadrupole interactions between the –OH group of simplified carbohydrate monomers and gas molecules were considered as typical initial structures for optimization (Figures S7-8). All interaction energies were estimated as the difference between the total energy of the monomer–gas complex and the sum of the total energy of the minimum geometry of the monomer and gas molecule, and then rectified with the

standard counterpoise method of Boys and Bernardi.[22] As shown in Figure 3, the hydroxyl groups on C-6 in Glc-2 and Gal-2 preferentially form intramolecular hydrogen bonds and
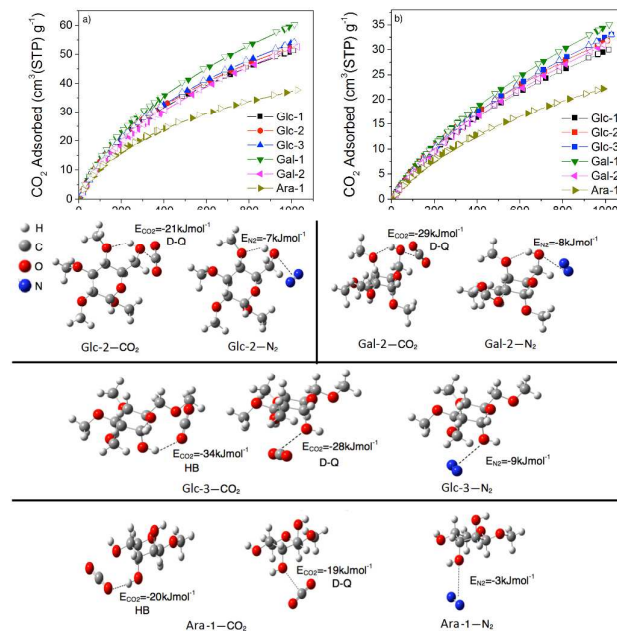

Figure 2. CO_2 adsorption (solid symbols)–desorption isotherms (open symbols) of samples up to 1.01bar at 273 K (a) and 298 K (b).

Figure 3. Optimized simplified carbohydrate monomer-gas dimer structures obtained from quantum chemistry calculations. In this figure, HB represents hydrogen bonding and D-Q stands for dipole-quadrupole interactions.

interact with CO_2 by dipole–quadrupole interactions. In contrast, in Glc-3 and Ara-1, both hydrogen bonds and dipole–quadrupole interactions occur between the carbohydrate monomers and CO_2. This can explain why the secondary hydroxyl groups in Glc-3 can boost CO_2/N_2 selectivity when compared with the primary hydroxyl groups in Glc-2, especially under higher pressure in mixed gases or at higher temperature. Specifically, to achieve the most stable configuration, the primary hydroxyl groups in Glc-2 can only form relatively weaker dipole–quadrupole interactions with CO_2 (-21 kJ mol^{-1}). In contrast, stronger hydrogen bonding between the –OH groups and CO_2 (-34 kJ mol^{-1}) enhances the carbon capture performance of Glc-3. In addition, Gal-2 has a stronger affinity with CO_2 than Glc-2 (-29 kJ mol^{-1} vs. -21 kJ mol^{-1}), in line with the higher CO_2/N_2 selectivity of Gal-2 obtained experimentally. Generally, the CO_2/N_2 selectivity is determined by both the CO_2-philic and N_2-phobic properties of chemical functional groups in MOPs. For the –OH groups on C-2, 3, 4 of Ara-1, both their hydrogen bonding and dipole–quadrupole interactions with CO_2 are moderate, but their interactions with N_2 are extremely low (approximately -3 kJ mol^{-1}). These N_2-phobic hydroxyl groups also serve to enhance the CO_2/N_2 selectivity of Ara-1 compared to Glc-2.

Conclusions

In summary, we have designed and synthesized a series of novel carbohydrate-based microporous organic polymers by

hypercross-linking various hydroxyl-functionalized carbohydrate monomers with the cross-linker FDA. We have also explored and demonstrated that several factors, including quantity and reactivity of hydroxyl groups and the structure of the carbohydrate monomers all contribute to the CO_2 adsorption. In general, these carbohydrate-based polymers show robust microporous structures, good thermal stability, high surface area, respectable CO_2 uptake and competitive adsorption selectivity for CO_2 over N_2. Moreover, the green chemistry nature of these carbohydrate-based polymers makes them amenable to solve environmental issues like CO_2 absorption, and we hope these promising microporous polymers will find broad applications in carbon capture.

Acknowledgements

Notes and references

1   M. Abolhasani, A. Gunther, E. Kumacheva, *Angew. Chem. Int. Ed.*, 2014, **53**, 7992.
2   D. W. Keith, *Science*, 2009, **325**, 16544.
3   (a) R. Dawson, D. J. Adams, A. I. Cooper, *Chem. Sci.*, 2011, **2**, 1173; (b) J. Wang, L. Huang, R. Yang, Z. Zhang, J. Wu, Y. Gao, Q. Wang, D. O'Hare, Z. Zhong, *Energy Environ. Sci.*, 2014, **7**, 3478.
4   (a) S. Fischer, J. Schmidt, P. Strauch, A. Thomas, *Angew. Chem. Int. Ed.*, 2013, **52**, 12174; (b) R. Dawson, E. Stockel, J. R. Holst, D. J. Adams, A. I. Cooper, *Energy Environ Sci.*, 2011, **4**, 4239; (c) X. Zhu, S. M. Mahurin, S-H. An, C-L. Do-Thanh, C. Tian, Y. Li, L. W. Gill, E. W. Hagaman, Z. Bian, J-H. Zhou, J. Hu, H. Liu, S. Dai, *Chem. Commun.*, 2014, **50**, 7933; (d) A. P. Katsoulidis, M. G. Kanatzidis, *Chem. Mater.*, 2011, **23**, 1818; (e) S. Xu, Y. Luo, B. Tan, *Macromol. Rapid Commun.*, 2013, **34**, 471.
5   M. R. Liebl, J. Senker, *Chem. Mater.*, 2013, **25**, 970.
6   (a) R. Dawson, L. A. Stevens, T. C. Drage, C. E. Snape, M. W. Smith, D. J. Adams, A. I. Cooper, *J. Am. Chem. Soc.*, 2012, **134**, 10741; (b) Y. Luo, B. Li, W. Wang, K. Wu, B. Tan, *Adv. Mater.*, 2012, **24**, 5703; (c) S. Xu, Y. Luo, B. Tan, *Macromol. Rapid Commun.*, 2013, **34**, 471; (d) S. Yao, X. Yang, M. Yu, Y. Zhang, J. Jiang, *J. Mater. Chem. A.*, 2014, **2**, 8054.
7   D. Wu, F. Xu, B. Sun, R. Fu, H. He, K. Matyjaszewski, *Chem. Rev.*, 2012, **112**, 3959.
8   X. Wang, O. Ramstrom, M. Yan, *Adv. Mater.*, 2010, **22**, 1946.
9   G. Mangiante, P. Alcouffe, B. Burdin, M. Gaborieau, E. Zeno, M. P-Conil, J. Bernard, A. Charlot, E. Fleury, *Biomacromolecules*, 2013, **14**, 254.
10 A. Varki, R. D. Cummings, J. D. Esko, H. H. Freeze, P. Stanley, C. R. Bertozzi, G. W. Hart, M. E. Etzler, *Essentials of Glycobiology*, Cold Spring Harbor Laboratory Press, Cold Spring Harbor, NY, 2nd edn, 2009.
11 F. Zhang, C. Liang, X. Wu, H. Li, *Angew. Chem. Int. Ed.*, 2014, **53**, 8498.
12 (a) S S. Shivatare, S-H. Chang, T-I. Tsai, C-T. Ren, H-Y. Chuang, L. Hsu, C-W. Lin, S-T. Li, C-Y. Wu, C-H. Wong, *J. Am. Chem. Soc.*, 2013, **135**, 15382; (b) L. Li, Y. Xu, I. Milligan, L. Fu, E. A. Franckowiak, W. Du, *Angew. Chem. Int. Ed.*, 2013, **52**, 13699.
13 J. Wei, L. Zheng, X. Lv, Y. Bi, W. Chen, W. Zhang, Y. Shi, L. Zhao, X. Sun, F. Wang, S. Cheng, J. Yan, W. Liu, X. Jiang, G. F. Gao, X. Li, *ACS Nano*, 2014, **5**, 4600.
14 J. J. Gassensmith, H. Furukawa, R. A. Smaldone, R. S. Forgan, Y. Y. Botros, O. M. Yaghi, J. F. Stoddart, *J. Am. Chem. Soc.*, 2011, **133**, 15312.
15 A. Thomas, *Angew. Chem. Int. Ed.*, 2010, **49**, 8328.
16 They proposed it based on the well-established principle that reactivity of primary hydroxyl groups is higher than secondary hydroxyl groups.
17 (a) R. A. Smaldone, R. S. Forgan, H. Furukawa, J. J. Gassensmith, A. M. Z. Slawin, O. M. Yaghi, J. F Stoddart, *Angew. Chem. Int. Ed.*, 2010, **49**, 8630; (b) R. S. Forgan, R. A. Smaldone, J. J. Gassensmith, H. Furukawa, D. B. Cordes, Q. Li, C. E. Wilmer, Y. Y. Botros, R. Q. Snurr, A. M. Z. Slawin, J. F. Stoddart, *J. Am. Chem. Soc.*, 2012, **134**, 406; (c) D. Wu, J. J. Gassensmith, D. Gouvea, S. Ushakov, J. F. Stoddart, A. Navrotsky, *J. Am. Chem. Soc.*, 2013, **135**, 6790; (d) J. J. Gassensmith, J. Y. Kim, J. M. Holcroft, O. K. Farha, J. F. Stoddart, J. T. Hupp, N. C. Jeong, *J. Am. Chem. Soc.*, 2014, **136**, 8277.
18 (a) G. J. L. Bernardes, E. J. Grayson, S. Thompson, J. M. Chalker, J. C. Errey, F. E. Oualid, T. D. W. Claridge, B. G. Davis, *Angew. Chem. Int. Ed.*, 2008, **47**, 2244; (b) E. Sasaki, C-I. Lin, K-Y. Lin, H-W. Liu, *J. Am. Chem. Soc.*, 2012, **134**, 17432.
19 B. Li, R. Gong, W. Wang, X. Huang, W. Zhang, H. Li, C. Hu, B. Tan, *Macromolecules*, 2011, **44**, 2410.
20 Y. Zhao, D. G. Truhlar, *Theor. Chem. Acc.*, 2008, **120**, 215.
21 M. J. Frisch, G. W. Trucks, H. B. Schlegel, G. E. Scuseria, M. A. Robb, J. R. Cheeseman, G. Scalmani, V. Barone, B. Mennucci, G. A. Petersson, H. Nakatsuji, M. Caricato, X. Li, H. P. Hratchian, A. F. Izmaylov, J. Bloino, G. Zheng, J. L. Sonnenberg, M. Hada, M. Ehara, K. Toyota, R. Fukuda, J. Hasegawa, M. Ishida, T. Nakajima, Y. Honda, O. Kitao, H. Nakai, T. Vreven, J. A. Montgomery, J. E. Jr. Peralta, F. Ogliaro, M. Bearpark, J. J. Heyd, E. Brothers, K. N. Kudin, V. N. Staroverov, T. Keith, R. Kobayashi, J. Normand, K. Raghavachari, A. Rendell, J. C. Burant, S. S. Iyengar, J. Tomasi, M. Cossi, N. Rega, J. M. Millam, M. Klene, J. E. Knox, J. B. Cross, V. Bakken, C. Adamo, J. Jaramillo, R. Gomperts, R. E. Stratmann, O. Yazyev, A. J. Austin, R. Cammi, C. Pomelli, J. W. Ochterski, R. L. Martin, K. Morokuma, V. G. Zakrzewski, G. A. Voth, P. Salvador, J. J. Dannenberg, S. Dapprich, A. D. Daniels, O. Farkas, J. B. Foresman, J. V. Ortiz, J. Cioslowski, D. J. Fox, Gaussian, Inc., Wallingford CT, 2010.
22 S. F. Boys, F. Bernardi, *Mol. Phys.*, 1970, **19**, 553.